Original Research Article

Determining soil conservation strategies: Ecological risk thresholds of arsenic and the influence of soil properties

Yihang Huang [a,b], Naichi Zhang [a,c], Zixuan Ge [d], Chen Lv [d], Linfang Zhu [a,c], Changfeng Ding [a], Cun Liu [a], Peiqin Peng [b], Tongliang Wu [a,*], Yujun Wang [a,c,*]

[a] State Key Laboratory of Soil and Sustainable Agriculture, Institute of Soil Science, Chinese Academy of Sciences, Nanjing 210008, China
[b] College of Environmental Science and Engineering, Central South University of Forestry and Technology, Changsha 410004, China
[c] University of Chinese Academy of Sciences, Beijing 100049, China
[d] College of Environmental Science and Engineering, Yangzhou University, Yangzhou 225009, China

ARTICLE INFO

ABSTRACT

The establishment of ecological risk thresholds for arsenic (As) plays a pivotal role in developing soil conservation strategies. However, despite many studies regarding the toxicological profile of As, such thresholds varying by diverse soil properties have rarely been established. This study aims to address this gap by compiling and critically examining an extensive dataset of As toxicity data sourced from existing literature. Furthermore, to augment the existing information, experimental studies on As toxicity focusing on barley-root elongation were carried out across various soil types. The As concentrations varied from 12.01 to 437.25 mg/kg for the effective concentrations that inhibited 10% of barley-root growth (EC_{10}). The present study applied a machine-learning approach to investigate the complex associations between the toxicity thresholds of As and diverse soil properties. The results revealed that Mn-/Fe-ox and clay content emerged as the most influential factors in predicting the EC_{10} contribution. Additionally, by using a species sensitivity distribution model and toxicity data from 21 different species, the hazardous concentration for x% of species (HCx) was calculated for four representative soil scenarios. The HC5 values for acidic, neutral, alkaline, and alkaline calcareous soils were 80, 47, 40, and 28 mg/kg, respectively. This study establishes an evidence-based methodology for deriving soil-specific guidance concerning As toxicity thresholds.

1. Introduction

Arsenic (As), a heavy metal widely distributed in the environment, is classified as a Group-1 carcinogen [1]. As-contaminated soil is globally widespread and presents a significant risk to human health through water and food consumption [2,3]. In addition, As has negative effects on the ecological processes within soils, such as impairing plant root and shoot growth [4] and causing acute lethality in soil invertebrates [5]. Therefore, establishing standards for monitoring As in soil ecosystems can profoundly enhance the management of As contamination, conservation of biodiversity, and preservation of soil health [6]. It provides guidance for policymakers, researchers, and land managers in evaluating and mitigating the adverse effects of heavy metals, including As, and promoting sustainable soil management practices [7]. Several countries have set specific environmental quality standards for As for various proposes: China has implemented screening values of

20–60 mg/kg for development land and 20–40 mg/kg for agricultural land. Similarly, the United States has set a screening value of 18 mg/kg for plants, and Canada has established a screening value of 12 mg/kg for agricultural and industrial land. The rational setting of soil quality standards requires appropriate thresholds for soil contaminants [8]. However, the availability and toxicity of As in soil can be significantly impacted by soil properties, which may have profound effects on the structure and function of soil ecosystems, ultimately affecting the ecological threshold for As [9,10].

The bioavailability and toxicity of As in soils can be strongly regulated by physicochemical properties that influence As speciation, solubility, and mobility. In particular, As exists predominantly as inorganic As(III) and As(V) species [11]. Factors such as pH, clay, soil organic matter (SOM), and Fe/Mn oxides play a vital role in the redox transformation and adsorption of As species, which was closely related to their availability and mobility [12,13]. A variety of statistical approaches can be

---

* Corresponding authors.
E-mail addresses: tlwu@issas.ac.cn (T. Wu), yjwang@issas.ac.cn (Y. Wang).

used to quantitatively analyze the relationships between inherent soil properties and contaminant toxicity. Common statistical approaches include empirical linear regression, correlation analyses, and path analysis [14–16]. Recently, machine learning (ML), a powerful tool for uncovering hidden and non-linear relationships among variables, has seen a growing application in environmental research, offering valuable insights into understanding environmental issues [17,18]. To date, the complex interactions between the ecological toxicity of As and soil-properties-based ML analysis have rarely been investigated.

Ecological risk thresholds for metal(loid)s in soils are commonly extracted from limited toxicological data of plants and invertebrate species. Whole ecosystem-level guidance values are then estimated using statistical extrapolation techniques such as species sensitivity distributions (SSDs) [19]. Generally, the protection level is defined based on the percentage of protected species and the SSD curve, whereas HC5 values are often chosen as the threshold in ecological risk assessment, representing the concentration at which 95% of species are protected [20,21]. In the recent years, the SSD method has been increasingly adopted in the study of soil environmental thresholds due to its ecological and statistical significance for calculating HC5 values [22]. SSD curves are usually fitted by Burr type III, log-logistic, log-normal, Weibull, and Gompertz distributions. The choice of model depends on the confidence level of the data [23].

This study derived site-specific ecological risk thresholds for As contamination in soils through integrated analysis of multiple online data sources and experimental results. Specifically, toxicological data were compiled from the literature on the adverse effects of As on plants, invertebrates, and microorganisms across species and soil types, along with original dose–response toxicity bioassays measuring As inhibition of plant root elongation across soils of different properties. This study aimed to (1) identify the key factors in controlling the As toxicity to barely by traditional and ML methods and (2) derive ecological risk thresholds for different land types based on ecological safety.

2. Material and methods

2.1. Soil samples

Twelve surface soil samples (0–20 cm) representing the major soil types from various provinces of China were collected. After air drying, soil samples were removed from plant residues, roots, and pebbles and then sieved for at least 2 mm to determine physiochemical properties. The properties of soil samples were measured using standard procedures. The pH and electrical conductivity (EC) were measured in purified water in 1:2.5 (w/v) and 1:5 (w/v) soil–water suspensions, respectively. SOM and cation exchange capacity (CEC) were measured by the dichromate method for the <100-mesh fraction [24] and ethylenediamine tetraacetic acid–ammonium acetate exchange method for the <100-mesh fraction [25], respectively. The pipette method was used to determine the clay content in soil samples by using a 10-mesh sieve [26]. Total inorganic carbon was determined using the high-temperature loss-on-ignition method after the addition of HCl to remove carbonates on the <20-mesh fraction (Leco TruMac CNS analyzer, USA). The amorphous Fe, Al, and Mn (Fe-ox, Al-ox and Mn-ox, respectively) were measured using the ammonium oxalate–oxalic acid (pH 3.0) in the dark, whereas the crystalline Fe, Mn, and Al (Fe-dithionite-citrate-bicarbonate [DCB], Al-DCB, and Mn-DCB, respectively) were measured using DCB. The total of nitrogen was measured by semi-micro-kjeldahl method on the <20-mesh fraction [27]. A summary of soil properties of twelve soils is listed in Table 1.

2.2. Experimental design

2.2.1. Aging experiment

In this study, all soils were spiked with As(V) (Na$_2$HAsO$_4$·7H$_2$O) at concentrations ranging from 0 to 1,000 mg/kg, depending on the soil pH.

For acidic soils, 0, 250, 500, 750, and 1,000 mg/kg were added, whereas for alkaline soils, 0, 200, 400, 600, and 800 mg/kg were added. The soils were incubated for 3 months at water contents of approximately 70% (w/w) of field capacity before experimentation. Prior to the toxicity experiments, the soils were air-dried, sieved, and mixed again. For each treatment in each soil, 400 g of air-dried soil was transferred to a polyvinyl chloride tube (7.5 cm × 14 cm), and deionized water was added to achieve 70% water-holding capacity.

2.2.2. Toxicity assay

The test to investigate the toxicity of barely-root elongation to As was conducted in accordance with ISO 11269–1:2012 in twelve soils. To prepare for the barley-root-elongation test, MengMai No.11 barley seeds were washed in 0.5% NaClO for 15 min and then washed with deionized water eight times. The seeds were then allowed to germinate for 24 h at 25 °C on wet filter paper in a Petri dish. Seeds with root elongation of between 1 and 2 mm were chosen for the test. Each tube held five seeds, which were then covered with 1 cm of soil. All tubes were placed in an artificial-climate chamber with preset growth conditions (14 h of light at 25 °C and 10 h of darkness at 18 °C, with a light intensity of 24,000 lx). To keep the water-holding capacity at 70%, deionized water was added every day. After four days of growth, the plants were carefully removed from the tubes and washed repeatedly with deionized water. Additionally, Mollisol from Jilin (S5), and Ultisol from Jiangxi (S12) as two representative soils to grow 12 plants, including leafy (Bok choy [*Brassica rapa chinensis*], Lettuce [*Lactuca sativa*], Water spinach [*Ipomoea aquatica*], Amaranthus [*Amaranthus tricolor*]), solanaceous vegetables (Loofah [*Luffa aegyptiaca*], Cucumber [*Cucumis sativus*], Radish [*Raphanus sativus*], Zucchini [*Cucurbita pepo*]), and landscape plants (Crpress vine [*Ipomoea quamoclit*], Lavandula [*Lavandula angustifolia*], Zinnia [*Zinnia elegans Jacquin*], Sunflower [*Helianthus annuus*]). These phytotoxicity assays were similar to these barley-root-elongation experiments but with extended exposure durations of 5 days to account for differential growth rates. The S5 and S12 were selected for detailed investigation because they exhibited notable differences in key properties known to influence heavy-metal toxicity thresholds. Specially, S12 had a pH of 4.55 and SOM content of 15.48 g/kg, whereas S5 had a pH of 7.62 and higher SOM content of 30.33 g/kg. Significant differences were also observed in EC and Fe, Mn, and Al contents between the two soils (Table 1). Furthermore, the S12 and S5 represent the range of cultivated agricultural soils found across major rice-growing (Jiangxi) and wheat-growing (Jilin) regions in China.

2.2.3. Extraction of As in soils

In order to extract available As from aged soils, a sequential extraction procedure was proposed by Wenzel et al. [28]. The first two steps of this procedure involved using NH$_4$H$_2$PO$_4$ (0.05 M) as the extractant. Two gram of soil was mixed with 25 mL of the extractant and shaken at room temperature for 16 h. Following this, the samples were centrifuged at 5,000 rpm for 15 min, and the resulting supernatants were filtered through a 0.45-μm membrane filter. The concentrations of As in the extracts were then determined using atomic fluorescence spectrometry.

2.3. Normalize and analyze toxicity data

2.3.1. Dose–response curves fitting

The elongation of roots was recorded, and relative root elongation (RRE, %) was calculated by the following equation (Eq. 1):

$$RRE = (RE_T / RE_{C0}) \times 100\% \tag{1}$$

where RE$_T$ and RE$_{C0}$ are the barley-root elongation in soils with and without As addition, respectively.

The dose–response data were fitted by logistic curve as follows (Eq. 2):

Table 1
Basic properties of soils.

No.	Site	Classification	pH	SOM g/kg	EC μs/cm	TN g/kg	TIC g/kg	Clay %	CEC cmol/kg	Fe-ox Fe, g/kg	Mn-ox Mn, g/kg	Al-ox Al, g/kg	Fe-DCB Fe$_2$O$_3$, g/kg	Mn-DCB MnO, g/kg	Al-DCB Al$_2$O$_3$, g/kg
S1	Zhejiang	Alfisol	4.46	31.09	40.41	1.51	0.80	30.60	10.95	4.19	0.79	2.94	28.13	1.25	3.20
S2	Hainan	Oxisol	5.78	25.77	43.77	1.38	0.66	62.90	12.11	2.76	1.57	1.42	127.73	2.17	18.78
S3	Hebei	Inceptisol	8.45	13.67	138.10	1.05	2.92	17.70	11.08	0.71	0.22	0.53	9.93	0.27	1.67
S4	Heilongjiang	Mollisol	5.80	48.17	108.70	2.31	0.50	33.30	34.14	2.91	0.44	1.84	8.95	0.56	3.54
S5	Jilin	Mollisol	7.62	30.33	91.90	1.66	1.01	32.30	29.01	1.52	0.56	1.52	10.03	0.73	2.34
S6	Jiangsu	Alfisol	7.20	16.40	57.70	1.01	1.05	11.70	9.30	1.84	0.07	0.47	7.47	0.10	2.31
S7	Shaanxi	Mollisol	8.09	17.00	140.60	1.12	7.49	24.40	12.01	0.74	0.28	0.73	12.95	0.41	1.84
S8	Sichuan	Alfisol	8.13	14.95	161.70	1.05	7.31	35.00	22.61	1.62	0.27	0.62	11.44	0.47	2.37
S9	Guangdong	Ultisol	4.94	23.50	73.67	1.26	0.56	19.10	6.50	3.38	0.04	0.82	7.59	0.05	1.77
S10	Chongqing	Entisol	5.09	13.02	26.24	0.86	0.78	25.00	12.93	2.46	0.22	0.71	16.72	0.31	2.97
S11	Hubei	Ultisol	6.61	18.76	60.21	1.17	0.86	28.20	9.15	2.66	1.12	0.75	24.40	1.54	3.58
S12	Jiangxi	Ultisol	4.55	15.48	43.72	1.02	0.53	49.60	11.73	2.05	0.09	1.99	39.1	0.24	6.35

CEC, cation exchange capacity; DCB, dithionite-citrate-bicarbonate; EC, electrical conductivity; SOM, soil organic matter; TIC, total inorganic carbon; TN, total nitrogen.

$$y = (A_1 − A_2)/[1 + (x/x_0)^p] + A_2 \qquad (2)$$

where y is the relative root elongation (%), x is the spiked As concentration (mg/kg), and x_0 is the half-maximal effective concentration (EC$_{50}$) (mg/kg). A_1, A_2, and p are the parameters to be fitted. The EC$_{10}$, EC$_{20}$, and EC$_{50}$ were obtained after fitting, indicating 10%, 20%, or 50% of inhibition effects on barley-root elongation, respectively.

2.3.2. Screening of toxicological data and normalization of As ecotoxicity data

In this study, a toxicity data search was conducted in Web of Science to identify toxicity studies related to As in soil. Literature collection was carried out based on the following requirements: (1) As contamination was caused by exogenous addition and relevant soil properties were provided; (2) test endpoints were based on plants, invertebrates, and microorganisms; (3) EC$_{10}$ were directly provided or inferred from original data; and (4) experiments used standardized experimental methods and procedures. Ultimately, toxicity data for 9 species were collected.

Due to the lack of sufficient toxicity data, some species may not be able to build As ecotoxicity prediction models and, therefore, have to use the same prediction model as for other species. In general, toxicity data were obtained from different soils of varying characteristics. A cross-species extrapolation of results was built upon the assumption that the slopes of the parameters (a and b) remained consistent between plant species, indicating soil properties exerted a uniform influence on metal toxicity to plants. Only the intrinsic sensitivity parameter (k) was presumed to vary between species [29]. The normalized approach in this study was based on an empirical prediction model between As toxicity data and basic soil properties. The predictive model for EC$_{10}$ toxicity of As in soils is typically given by Eq. 3:

$$\log[EC_{10}] = a \times pH + b \times \log[clay] + k \qquad (3)$$

where EC$_{10}$ is the biologically inhibited 10% concentration, a and b are the slopes of the soil properties, and k is the intrinsic sensitivity of the species.

The normalized EC$_{10nor}$ equation:

$$EC_{10nor} = EC_{10} \times 10^{a \times (pHnor-pH)+b \times (\log[claynor]-\log[clay])} \qquad (4)$$

where EC$_{10}$ is the biologically inhibited 10% concentration, a and b are the slopes of the soil properties, and "nor" is the corresponding target normalization parameter.

2.3.3. SSD construction and HC5 values derivation

The SSD curves and HC5 values were estimated using the Burr Type III distribution fitted with BurrliOZ software (version 1.0.14, CSIRO, Australia). The Burr III function is a flexible three-parameter distribution well suited for approximating other commonly used distributions. The Burr Type III distribution is defined by the following equation:

$$y = \frac{1}{\left[1 + \left(\frac{b}{x}\right)^c\right]^k} \qquad (5)$$

where b, c, and k are the three parameters. When k and c approach infinity, the Burr Type III distribution approaches the ReWeibull and RePareto distributions, respectively [29].

2.4. Influencing factors identification

2.4.1. Traditional statistic methods

The correlation and regression analysis between EC$_{10}$ and soil properties were conducted by SPSS (version 18) (SPSS, Chicago, IL). The aggregate-boosting trees (ABT) model was performed through the gbmplus package in R language [30].

2.4.2. Machine-learning method

Research methods in studies addressing the effects of soil properties on the toxicity of heavy metals are mostly based on correlation analysis, ordinary linear regression, and empirical models, which are traditionally limited either by the number of properties considered or by the influence factors based on subjective assumptions [31]. ML methods do not rely on hypothetical mechanisms to discover data and can accurately identify relationships between input and output variables from data and provide predictive models by learning input variables and predicting target values [32]. Although ML methods have been widely used in environmental field research, they are still very limited due to data or input variables [18]. To address this gap, we used a gradient-boosting regression tree (GBRT) model to develop a predictive model for EC_x of As.

During the modeling, the input data consisted of soil pH, OM, clay, CEC, Fe-ox, Mn-ox, and Al-ox. The output variables were the toxicity thresholds for barley root elongation, specifically EC_{10} and EC_{50}. The procedure of the GBRT model development included (1) unifying the units of each variable; (2) transforming the input (except pH) and target into the logarithm form; (3) splitting the data into training and test set in the ratio of 8:2; (4) tuning the hyperparameters, including learning rate, max depth and the number of estimators, by Bayesian optimization during 5-fold cross-validation on training set; and (5) quantifying the model performance based on R^2 (coefficient of determination).

Based on the optimal GBRT model, three feature analysis methods were applied to assess feature importance and the relationships between descriptors and targets. The SHapley Additive exPlanation method, based on coalitional game theory, is wildly used to explain how certain features influence its output in a black-box model. Partial dependence plots (PDPs) and two-dimensional interactions PDPs were used to provide systematic explanations of the correlation between the descriptors of interest and the output variable.

3. Results

3.1. Soil characteristics

As shown in Table 1, the 12 test soils exhibited a wide range of physicochemical properties important for As toxicity assessments. Specifically, soil pH varied from 4.46 to 8.45. Clay content also showed significant diversity, ranging from 11.7% to 62.9%. Regarding soil minerals influencing As bioavailability, higher Fe-ox contents (2.91–4.19 g/kg) in the soils from Zhejiang (S1), Heilongjiang (S4), and Guangdong (S9) were found in comparison to 0.71–2.76 g/kg in others. Similarly, Mn-ox levels in soils from Zhejiang (S1), Hainan (S2), and Hubei (S11) of 0.79–1.57 g/kg were higher than that in other soils (0.04–0.56 g/kg). Wu et al. [33] analyzed 12 soils and found that when pH ranged from 4.91 to 8.25, SOM content ranged from 7.9 to 46.1 g/kg, Fe-ox content ranged from 0.52 to 7.87 g/kg, and Mn-ox ranged from 0.02 to 0.55 g/kg. Meanwhile, Huang et al. [34] characterized 18 soils across China and reported that when pH ranged from 4.62 to 8.69, SOM content ranged from 5.7 to 81.1 g/kg, and clay content ranged from 10.4% to 61.8%. Therefore, the physicochemical properties of soils from the same regions in this study fell within the ranges outlined in previous work, suggesting that our test soils adequately represented conditions reported nationally.

3.2. Toxicity of As on barley root elongation model

3.2.1. Dose–response curve

The log-logistic model was used to fit the dose–response curves of results collected from various test endpoints in the 12 soil samples (Fig. S1). The inhibition of barley-root elongation and toxicity thresholds (EC_{10}, EC_{20}, and EC_{50}) varied significantly between soils. The EC_{10}, EC_{20}, and EC_{50} were 12.01–437.25, 21.71–481.47, and 59.75–678.26 mg/kg, respectively (Table S1). The Inceptisol (S3) exhibited the lowest EC_{10},

EC_{20}, and EC_{50} (EC_{10}: 12.01 mg/kg; EC_{20}: 21.71 mg/kg; EC_{50}: 59.75 mg/kg). In contrast, the Oxisol (S2) exhibited the highest EC_{10} and EC_{20} (EC_{10}: 437.25 mg/kg; EC_{20}: 481.47 mg/kg) and the Alfisol (S1) exhibited the highest EC_{50} (EC_{50}: 678.26 mg/kg).

3.2.2. Influence of soil properties on As toxicity thresholds

To obtain more reliable results, a correlation analysis was conducted by integrating toxicological data from Song et al. [35] and this experiment based on barley-root elongation (Fig. 1a). The combined results indicated that Mn-ox, Al-ox, and clay were the primary factors affecting EC_{10}, as well as the results from this experiment (Fig. S2), which could be confirmed by ABT analysis (Fig. 1b). Stepwise multiple linear regression analysis was applied to derive optimal equations for predicting EC_{10} and EC_{50}, based on soil properties. Mn-ox was identified as a significant factor in elucidating the variability in both EC_{10} and EC_{50}. The resulting regression equations accounted for 68.9% of the variation in EC_{10} and 63.0% of the variation in EC_{50} when Fe-ox was added to the equations (Table S2).

To further explore the intricate relationships between the toxicity thresholds of As and various soil properties, ML methods were conducted. A comprehensive dataset was also constructed by combining the results of this experiment and Song's results [35] to predict the EC_x of As. The prediction results from the optimal GBRT model are shown in Fig. 1 and S4. For EC_{10}, the training and test R^2 were 0.95 and 0.67, respectively, and for EC_{50}, the training and test R^2 were 0.99 and 0.65, respectively (Fig. S3).

Based on the optimal GBRT model, the role of the final feature concerning the output EC_x was explored using both the GBRT explainer and SHAP methods (Fig. 1d, Fig. S4a). Specifically, high SHAP values imply that the corresponding input features have a greater impact on model predictions. The two most important features used to predict the contribution of EC_{10} were soil clay and Mn-ox, whereas Fe-ox and pH also had an impact on EC_{10} prediction (Fig. 1e). The remaining properties, including CEC, SOM, and Al-ox, showed less potency in predicting the EC_{10} in the following order: CEC > SOM > Al-ox. Similarly, the importance of features involved in EC_{50} was in the following order: clay > Fe-ox > Mn-ox > pH > CEC > Al-ox > SOM (Fig. S4).

Based on the results of the SHAP analysis, this study extracted the four most important features to investigate their intrinsic correlation with EC_x. The PDPs with ICEs subplots thoroughly elaborated the correlation of these four features with the output variables (Figs. 1 and S4). It was observed that clay and Fe-ox showed a fluctuating upward trend with both EC_{10} and EC_{50}, indicating that higher values of these variables were associated with higher toxicity thresholds (Fig. 1f and 1h, Fig. S4c and S4d, Fig. S5). In addition, Mn-ox showed a significant positive contribution to EC_{10} and EC_{50} (Fig. 1g and Fig. S4e).

3.2.3. Bioavailability of As in soils

The availability of As was closely related to its toxicity and was assessed based on $NH_4H_2PO_4$ (0.05 M) single extraction. The extractable As accounted for 17.7%–65.2% of the total As content in soils among all treatments after aging for three months, and previous study has shown that the bioavailability of exogenous As in soil typically reaches equilibrium within approximately three months during the aging process [36]. Indeed, with similar conditions in this study, we found no significant differences in the bioavailability of As between 90 and 360 days of aging in the soils investigated. Extracted As concentration was higher with larger value of As added into soils and resulted in more obvious inhibition of root elongation. Similar results have been previously reported for As toxicity in soil, indicating that the available As could serve as a more accurate predictor of its toxicity in plants [37]. The relationship between barley-root elongation and extracted As concentration is exhibited in Fig. S6, showing a negative linear relationship (with a slope of −0.016) between the root elongation and As bioavailability, indicating obvious inhibition of bioavailable As to root elongation.
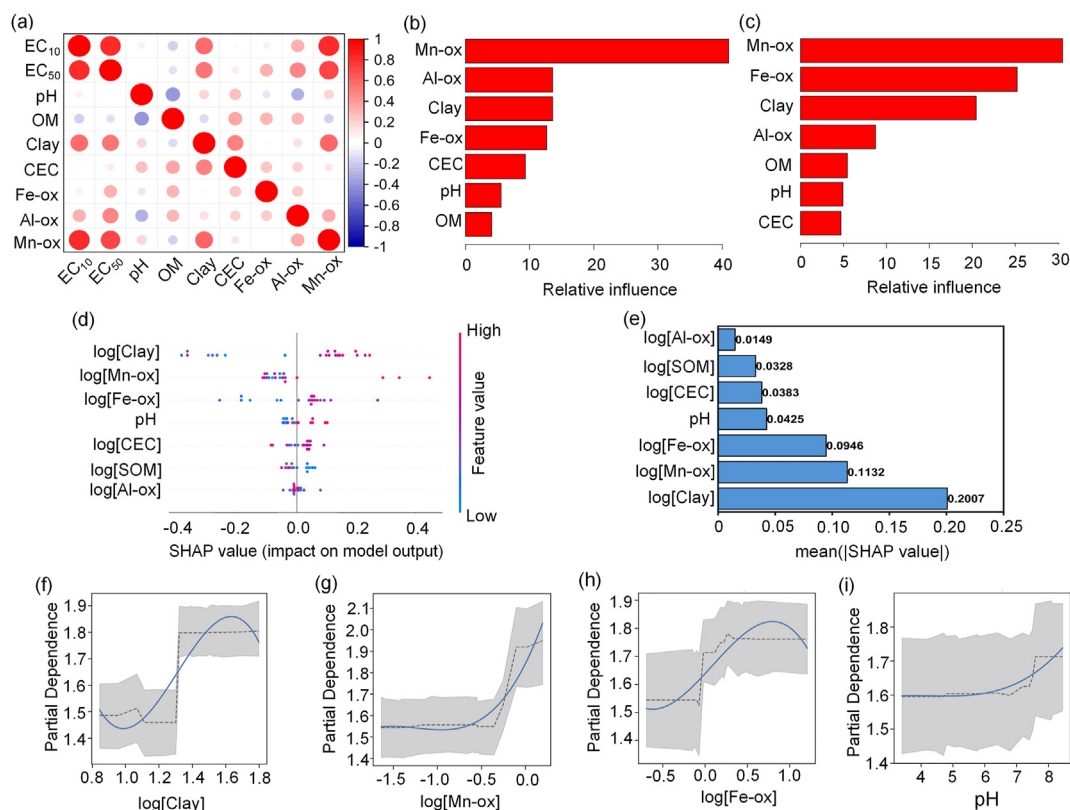
Fig. 1. (a) Correlation analysis between toxicity thresholds and soil properties, the relative contribution of soil properties to (b) EC_{10}, and (c) EC_{50}; (d and e) Shapley additive explanations (SHAP) values and the mean absolute Shapley for soil properties affecting EC_{10}; (f, g, h, i) PDPs analysis for clay, Mn-ox, Fe-ox, and pH affecting EC_{10}. PDP, partial dependence plot.

3.3. Ecological risk threshold for As

3.3.1. Normalization of toxicology data and establishment of database

The ML analysis identified soil pH, clay, and Fe-/Mn-ox as the primary predictors for As toxicity thresholds. However, Fe-/Mn-ox data were largely absent from the compiled literature during data screening, precluding its inclusion in predictive modeling across all studies. Therefore, to develop a more robust and generalizable model using commonly reported parameters, soil pH and clay content were selected as the independent variables for the toxicity prediction equation [38,39]. Two equations were derived (for barley and wheat) by normalizing the limited toxicological data available from laboratory experiments and literature (Table 2). The specific normalization process used is detailed in SI.

To validate the prediction equations, the study compared the predicted toxicity thresholds against the actual measured thresholds for each test species. The ratios between the predicted and actual toxicity

thresholds were found to be within a factor of 2 (Fig. 2). For each species, the prediction equation that resulted in a ratio closest to 1 between the predicted and measured thresholds was selected as the most accurate prediction model.

3.3.2. Species sensitivity of As in two representative soils

This study selected Mollisol from Jilin (S5) and Ultisol from Jiangxi (S12) as two representative soils to grow 12 plants, including leafy, solanaceous vegetables, and landscape plants. In S5 soil, the EC_{10} ranged from 100.17 to 353.7 mg/kg and EC_{50} ranged from 270 to 1,234.15 mg/kg. Meanwhile, in S12 soil, EC_{10} ranged from 140.41 to 723.96 mg/kg and EC_{50} ranged from 414.52 to 1,003.85 mg/kg (Table S3, Fig. S7). Besides, toxicity data of 9 species were collected, including plants, invertebrates, and microorganisms (Table S4), and plants generally exhibited the lowest sensitivities to As. The normalized EC_{10} of species in different soils are varied, with corn being the most sensitive to As toxicity in acidic and neutral soil and broad bean being

Table 2
The intrinsic sensitivity (k values) for non-model cultivars fitted by model from barley and wheat.

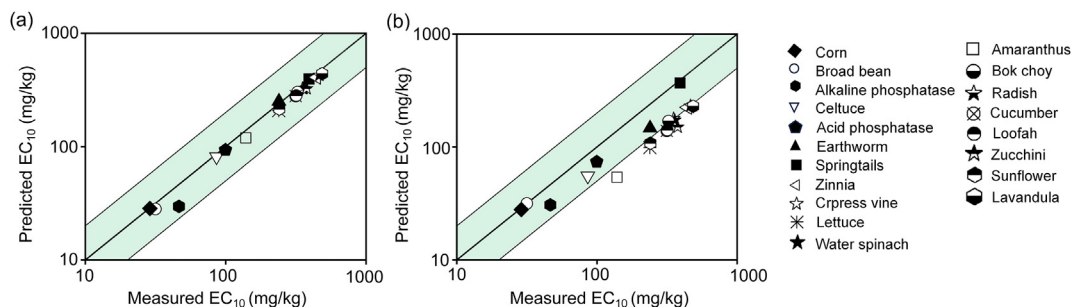| Species	Prediction equation	Cultivars	k	Cultivars	k
Barley (*Hordeum vulgare*)	$\log[EC_{10}] = -0.016\text{pH} + 0.343\log[\text{Clay}] + 1.69$	Corn (*Zea mays*)	1.19	Crpress vine (*Ipomea quamoclit*)	2.12
		Celtuce (*Lactuca sativa* var *augustana*)	1.71	Lettuce (*Lactuca sativa*)	1.92
		Earthworm (*Eisenia foetida*)	2.13	Water spinach (*Ipomea aquatica*)	2.12
		Acid phosphatase	1.63	Amaranthus (*Amaranthus tricolor*)	1.68
		Springtails (*Collembola*)	2.31	Bok choy (*Brassica rapa chinensis*)	2.08
		Zinnia (*Zinnia elegans Jacquin*)	2.22	Radish (*raphanus sativus*)	2.23
		Cucumber (*Cucumis sativus*)	2.05	Loofah (*Luffa aegyptiaca*)	2.05
		Zucchini (*Cucurbita pepo*)	2.12	Sunflower (*Helianthus annuus*)	1.94
		Lavandula (*Lavandula angustifolia*)	2.25		
Wheat (*Triticum*)	$\log[EC_{10}] = -0.16\text{pH} - 0.049\log[\text{Clay}] + 2.05$	Broad bean (*Vicia faba Linn*)	2.84		
		Alkaline phosphatase	2.94		

Fig. 2. Measured EC$_{10}$ versus predicted values from this study and the literature from (a) barley model and (b) wheat model. The solid line indicates the 2-fold prediction interval between the predicted and measured values.

the most sensitive species in alkaline and alkaline calcareous soil. Meanwhile, zucchini and springtails were the least sensitive species in the four representative scenario soils (Fig. 3).

3.3.3. The fit of SSD curve

The SSD curves for As in the four representative soil scenarios were constructed by fitting normalized ecotoxicity data with Burr Type III. The soil properties of four representative soil scenarios: acidic, neutral, alkaline, and alkaline calcareous soil are shown in Table S5 [40]. The plant height of corn and root elongation of broad bean are most sensitive to As toxicity, and the survival rate springtails are least sensitive to As toxicity. The HC5 values exhibited approximately a four-fold range across the four soil types evaluated, i.e., 80 mg/kg (acidic soil), 47 mg/kg (neutral soil), 40 mg/kg (alkaline soil), and 28 mg/kg (alkaline calcareous soil). The HC5 values decreased with increasing soil pH (Fig. 3).

The prediction models for HCx of four different land types were obtained by stepwise regression (Table S6), and the ecological risk thresholds of different land types with pH and clay were obtained by the predictive model (Table 3). The study reveals that the ecological risk thresholds for nature conservation and agricultural land are the most stringent, ranging from 32 to 82 mg/kg, whereas commercial and industrial land has relatively less stringent thresholds, ranging from 134 to 230 mg/kg. Furthermore, the ecological risk thresholds of alkaline soils are generally more stringent than for acidic soils. Meanwhile, this study derived HC5 values for S5 soil and S12 soil from Burr Type III based on the toxicity thresholds of 12 species planted on the two soils, and it was found that the HC5 value of S5 soil was 114 mg/kg, whereas that of S12 soil was 158 mg/kg (Fig. S8). The hazard concentrations for the different land types were also derived based on the two soils (Table S7).
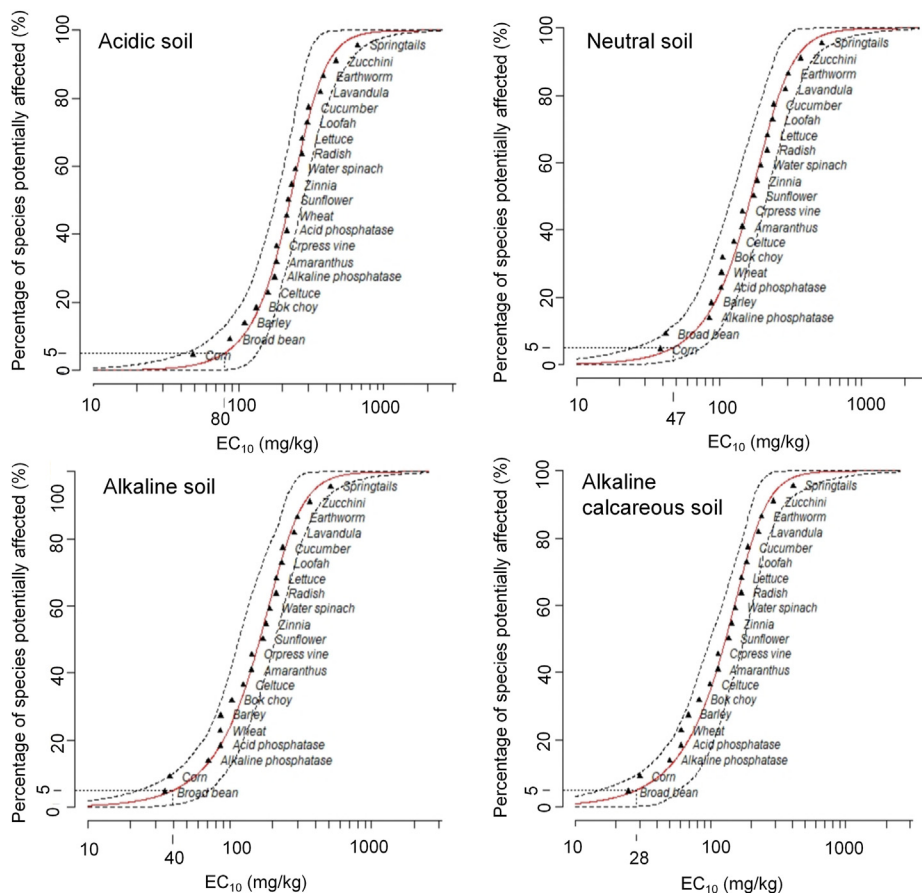

Fig. 3. Species sensitivity distribution of toxicity thresholds for 21 species in four representative soil scenarios.

Table 3
Ecological risk thresholds of total As in soils of different land types.

Land types	Hazard concentration	<5.5			5.5–6.5			6.5–7.5			>7.5		
		a	b	c	a	b	c	a	b	c	a	b	c
Nature conservation and agricultural land	HC5	64	75	82	51	59	65	40	47	52	32	37	41
Park land	HC20	115	133	145	99	115	125	85	99	108	74	85	93
Residential land	HC40	156	183	201	141	165	182	127	149	164	115	134	148
Commercial and industrial land	HC50	171	206	230	158	190	212	146	176	196	134	162	181

The thresholds at soil pH values of 5.0, 6.0, 7.0, and 8.0 were used for scenarios of soil pH <5.5, 5.5–6.5, 6.5–7.5, and >7.5, respectively.

a, b, and c were scenarios with soil clay contents of 20%, 40%, 60% respectively.

4. Discussion

4.1. Critical soil factors for As ecotoxicity

In this study, the toxicity thresholds of barley-root elongation were predicted by both traditional data analysis (correlation and regression analysis) and the ML method. The ML method showed that the main influencing factors for EC_{10} and EC_{50} were clay, Fe-/Mn-ox, and pH. Previous studies have indicated that the clay content and Mn oxides in soil are associated with the bioavailability of As [41]. Because of its layered structure and large surface area, clay is a natural adsorbent for As through inner-sphere complexation [42]. In addition, Fe (hydr)oxides, including goethite and ferrihydrite, could effectively immobilize As species [43,44], and it has been shown that As(V) is adsorbed by mononuclear bidentate corner-sharing with Fe oxides [45]. Oxidation and adsorption processes can significantly affect the environmental As mobility. Mn oxides are important adsorbents and oxidizers in soils as the –OH on Mn oxides can convert As(III) to less toxic As(V), and Mn oxides can adsorb As(V) via inner-sphere complexation at edge surface sites [46–48].

Similar results were obtained from the correlation analysis and linear regression, which revealed that Mn-ox has the greatest effect on EC_{10}, followed by Al-ox, Fe-ox, and clay. However, the effect of pH on EC_{10} was not significant in the correlation analysis. Indeed, ML analysis was able to reveal non-linear relationships that better capture their associations. Specifically, as shown in Fig. 1d, e, and i, the ML model uncovered a non-linear relationship between pH and EC_{10} values. Additionally, by analyzing feature interactions between pH, clay, and Fe oxides (Fig. S5), it was found that higher pH levels (pH > 7.5) combined with either high clay content (log[Clay] > 1.35) or high Fe oxides (log[Fe-ox] > 0.25) tended to increase EC_{10}.

Furthermore, there are additional factors that could impact As behavior in soils, including soil redox potential, microbial activity, and coexisting anion. Under reduced soil conditions, As(V) could be microbially reduced to the more toxic As(III) and then methylated into species such as monomethylarsenate and dimethylarsenate by sulfate-reducing bacteria [49,50], which could significantly alter their bioavailability and toxicity. However, the aging experiment in this study was conducted under oxic conditions, limiting the influence of redox-driven processes on As mobilization and toxicity. In addition, coexisting phosphate can compete with As for adsorption sites on soil particles, potentially affecting As bioavailability, as shown previously [51].

4.2. As toxicity to the ecosystem

Arsenic is a non-essential element for plant growth. Upon uptake, it interferes with metabolic processes, resulting in physiological and morphological abnormalities and retarded growth [52]. Due to similarities in chemical structure between arsenate and phosphate, phosphate transporters could facilitate the absorption and translocation of As within plants [53]. Once internalized, As binds to enzymes and proteins, disrupting normal metabolism. This metabolic disruption increases the production of reactive oxygen species, such as superoxide and hydroxyl radicals, in plant tissues. These free radicals induce oxidative stress through oxidation reactions, ultimately damaging cellular growth via oxidation-based damage [54,55].

Invertebrates are an essential component of the ecosystem and the main species in soil formation and organic matter decomposition [56]. In the past, the main indicators for invertebrate toxicity studies were survival, growth, and reproduction. These endpoints are usually insensitive. In recent years, studies have focused more on molecular endpoints because of their ability to respond sensitively, even in the presence of low concentrations of pollutants [57,58]. According to Wang et al. [59], under As stress, the amounts of superoxide dismutase, catalase, glutathione peroxidase, and glutathione s-transferase in earthworms would initially increase and then decrease, whereas malondialdehyde had a tendency to increase gradually. Although organic As shows less toxicity to organisms, it could be converted into highly toxic inorganic As under demethylation. Different forms of As have different toxicity effects on invertebrates, as evidenced by the finding that As(III) is more toxic than As(V) to earthworms at the molecular and subcellular levels, including oxidative damage, metallothionein induction and lysosomal membrane damage [60].

Microorganisms play an important role in soil geochemical cycling processes [61] and can alter the form of As in soil through redox, methylation–demethylation, and thus its availability [62]. However, microorganisms do not have specific As transport pathways since As is usually transported by phosphate pathways [63]. The toxic effect of As on soil enzyme activity could be altered by soil type, enzyme species, and arsenic valence. Urease activity was insensitive to As(V), but can be inhibited by high concentrations of As(III), whereas alkaline phosphatase activity was strongly inhibited by As(V) [64,65].

4.3. Toxicity thresholds and significance of HC5 values derivation

Various species tested in different soils exhibited diverse responses to As toxicity, and the derived EC_x values from different test endpoints for the same species exhibited significant variations [66,67]. Biological test endpoints are essential in determining the toxicity threshold [68]. In general, indicators of long-term or chronic toxicity of test species should be prioritized in the development of environmental quality criteria [69]. The toxic effects of As on different test endpoints varied significantly, and the toxicity data collected in this study varied in the selection of test endpoints by species, because indicators of toxicity have been shown to better represent the ecotoxicity of As when deriving ecological risk thresholds [68,70]. The SSD method has been demonstrated to be effective for determining ecological risk thresholds [71]. It is worth noting that the HC5 values obtained through the SSD curve do not imply that 5% of the species are "sacrificed", whereas 95% of the species are protected [72]. The current Chinese environmental quality standards for As thresholds range from 25 to 40 mg/kg for food safety. However, there are no specific ecological risk thresholds established for As in soil.

In this study, the ecological risk thresholds of different land types and the hazard concentration of two typical cultivated soils were obtained. The ecological risk thresholds were negatively correlated with pH and positively correlated with clay, ranging from 32 to 82 mg/kg. At the same time, the HC5 values derived for Mollisol (S5) and Ultisol (S12) were 114 and 158 mg/kg, respectively, which were more lenient than the ecological risk thresholds in four representative soil scenarios. This is due to the fact that the ecological risk thresholds were derived with more comprehensive toxicity data (including invertebrates and microorganisms) and were

normalized. Therefore, it is necessary to consider the relationship between the number and proportion of different species in an ecosystem.

However, due to the lack of leaching and aging models, the toxicity data collected in the literature were not corrected for leaching-aging in this study. In order to enhance the accuracy of toxicity data, future derivations of ecological risk thresholds require the correction of the leaching-aging model. In addition, further field validation should strengthen the confidence of the thresholds established in this study.

5. Conclusion

This study investigated the relationships between soil properties and As toxicity by combining ML methods and traditional data analysis. Soil pH, Mn/Fe oxides, and clay content were found to be the most influencing soil factors. Then ecologically relevant As thresholds tailored to different soil conditions were established, ranging from 32 to 82 mg/kg and varying considerably between soils. These thresholds were found to correlate negatively with soil pH but positively with clay content. Taken together, the findings in this study filled the gap between ecological risk thresholds of As and soil properties based on existing data set and additional experiments in this study, offering valuable guidance critical for environmental management and protection of soil ecosystems.

CRediT authorship contribution statement

Y.H.H.: experiment, conceptualization, data analysis, original draft preparation, and data curation. N.C.Z.: data analysis, original draft preparation. Z.X.G.: data analysis. C.L.: investigation. L.F.Z.: methodology. C.F.D., C.L.: review and editing. P.Q.P.: supervision. T.L.W.: conceptualization, methodology, formal analysis, investigation, writing–original draft, supervision, funding acquisition, writing–review and editing. Y.J.W.: supervision, funding acquisition.

Declaration of competing interests

The authors have declared no conflicts of interest.

Acknowledgment

Appendix A. Supplementary data

Supplementary data to this article can be found online at https://doi.org/10.1016/j.eehl.2024.02.007.

References

[1] J. Wang, C.F. Kerl, P. Hu, M. Martin, T. Mu, L. Brüggenwirth, et al., Thiolated arsenic species observed in rice paddy pore waters, Nat. Geosci. 13 (4) (2020) 282–287, https://doi.org/10.1038/s41561-020-0533-1.

[2] M.B. Shakoor, R. Nawaz, F. Hussain, M. Raza, S. Ali, M. Rizwan, et al., Human health implications, risk assessment and remediation of As-contaminated water: a critical review, Sci. Total Environ. 601 (2017) 756–769, https://doi.org/10.1016/j.scitotenv.2017.05.223.

[3] R.N. Ratnaike, Acute and chronic arsenic toxicity, Postgrad. Med. 79 (933) (2003) 391–396, https://doi.org/10.1016/j.scitotenv.2017.05.223.

[4] S.F. Ahmed, P.S. Kumar, M.R. Rozbu, A.T. Chowdhury, S. Nuzhat, N. Rafa, et al., Heavy metal toxicity, sources, and remediation techniques for contaminated water and soil, Environ. Technol. Innov. 25 (2022) 102114, https://doi.org/10.1016/j.eti.2021.102114.

[5] C.J. Langdon, T.G. Piearce, S. Black, K.T. Semple, Resistance to arsenic-toxicity in a population of the earthworm Lumbricus rubellus, Soil Biol. Biochem. 31 (14) (1999) 1963–1967, https://doi.org/10.1016/S0038-0717(99)00118-2.

[6] Q. Zhou, Y. Teng, Y. Liu, A study on soil-environmental quality criteria and standards of arsenic, Appl. Geochem. 77 (2017) 158–166, https://doi.org/10.1016/j.apgeochem.2016.05.001.

[7] Y. Li, X. Cheng, K. Liu, Y. Yu, Y. Zhou, A new method for identifying potential hazardous areas of heavy metal pollution in sediments, Water Res. 224 (2022) 119065, https://doi.org/10.1016/j.watres.2022.119065.

[8] Y. Wu, Q. Liu, J. Ma, W. Zhao, H. Chen, Y. Qu, Antimony, beryllium, cobalt, and vanadium in urban park soils in Beijing: Machine learning-based source identification and health risk-based soil environmental criteria, Environ. Pollut. 293 (2022) 118554, https://doi.org/10.1016/j.envpol.2021.118554.

[9] H. Ran, X. Deng, Z. Guo, Z. Hu, Y. An, X. Xiao, et al., Pollution characteristics and environmental availability of toxic elements in soil from an abandoned arsenic-containing mine, Chemosphere 303 (2022) 135189, https://doi.org/10.1016/j.chemosphere.2022.135189.

[10] C.K. Jain, I. Ali, Arsenic: occurrence, toxicity and speciation techniques, Water Res. 34 (17) (2000) 4304–4312, https://doi.org/10.1016/S0043-1354(00)00182-2.

[11] S. Awasthi, R. Chauhan, S. Srivastava, R.D. Tripathi, The journey of arsenic from soil to grain in rice, Front. Plant Sci. 8 (2017) 1007, https://doi.org/10.3389/fpls.2017.01007.

[12] S.C. Ying, B.D. Kocar, S.D. Griffis, S. Fendorf, Competitive microbially and Mn oxide mediated redox processes controlling arsenic speciation and partitioning, Environ. Sci. Technol. 45 (13) (2011) 5572–5579, https://doi.org/10.1021/es200351m.

[13] X. Cai, L.K. ThomasArrigo, X. Fang, S. Bouchet, Y. Cui, R. Kretzschmar, Impact of organic matter on microbially-mediated reduction and mobilization of arsenic and iron in arsenic (V)-bearing ferrihydrite, Environ. Sci. Technol. 55 (2) (2020) 1319–1328, https://doi.org/10.1021/acs.est.0c05329.

[14] J. Im, K. Yang, E.H. Jho, K. Nam, Effect of different soil washing solutions on bioavailability of residual arsenic in soils and soil properties, Chemosphere 138 (2015) 253–258, https://doi.org/10.1016/j.chemosphere.2015.06.004.

[15] S.B. Singh, P.K. Srivastava, Bioavailability of arsenic in agricultural soils under the influence of different soil properties, SN Appl. Sci. 2 (2020) 1–16, https://doi.org/10.1007/s42452-019-1932-z.

[16] S. Khan, M. Naushad, E.C. Lima, S. Zhang, S.M. Shaheen, J. Rinklebe, Global soil pollution by toxic elements: current status and future perspectives on the risk assessment and remediation strategies–A review, J. Hazard Mater. 417 (2021) 126039, https://doi.org/10.1016/j.jhazmat.2021.126039.

[17] S. Zhong, K. Zhang, M. Bagheri, J.G. Burken, A. Gu, B. Li, et al., Machine learning: new ideas and tools in environmental science and engineering, Environ. Sci. Technol. 55 (19) (2021) 12741–12754, https://doi.org/10.1021/acs.est.1c01339.

[18] K.N. Palansooriya, J. Li, P.D. Dissanayake, M. Suvarna, L. Li, X. Yuan, et al., Prediction of soil heavy metal immobilization by biochar using machine learning, Environ. Sci. Technol. 56 (7) (2022) 4187–4198, https://doi.org/10.1021/acs.est.1c08302.

[19] E. Smolders, K. Oorts, P. van Sprang, I. Schoeters, C.R. Janssen, S.P. McGrath, et al., Toxicity of trace metals in soil as affected by soil type and aging after contamination: using calibrated bioavailability models to set ecological soil standards, Environ. Toxicol. Chem. 28 (8) (2009) 1633–1642, https://doi.org/10.1897/08-592.1.

[20] P.A. Van Sprang, F.A.M. Verdonck, F. Van Assche, L. Regoli, K.A.C. De Schamphelaere, Environmental risk assessment of zinc in European freshwaters: a critical appraisal, Sci. Total Environ. 407 (20) (2009) 5373–5391, https://doi.org/10.1016/j.scitotenv.2009.06.029.

[21] P. Gao, Z. Li, M. Gibson, H. Gao, Ecological risk assessment of nonylphenol in coastal waters of China based on species sensitivity distribution model, Chemosphere 104 (2014) 113–119, https://doi.org/10.1016/j.chemosphere.2013.10.076.

[22] G.K. Frampton, S. Jänsch, J.J. Scott-Fordsmand, J. Römbke, P.J. Van den Brink, Effects of pesticides on soil invertebrates in laboratory studies: a review and analysis using species sensitivity distributions, Toxicol. Environ. Chem. 25 (9) (2006) 2480–2489, https://doi.org/10.1897/05-438R.1.

[23] S. Belanger, M. Barron, P. Craig, S. Dyer, M. Galay-Burgos, M. Hamer, et al., Future needs and recommendations in the development of species sensitivity distributions: estimating toxicity thresholds for aquatic ecological communities and assessing impacts of chemical exposures, Integrated Environ. Assess. Manag. 13 (4) (2017) 664–674, https://doi.org/10.1002/ieam.1841.

[24] R.K. Lu, Methods for Soil Agro-Chemistry Analysis, China Agricultural Science and Technology Press, Beijing, 2000.

[25] Y.J. Wang, T.T. Fan, P.X. Cui, Q. Sun, D.M. Zhou, C.B. Li, et al., Binding and adsorption energy of Cd in soils and its environmental implication for Cd bioavailability, Soil Sci. Soc. Am. J. 84 (2) (2020) 472–482, https://doi.org/10.1002/saj2.20034.

[26] M. Abdulaha-Al Baquy, J.-Y. Li, J. Jiang, K. Mehmood, R.-Y. Shi, R.-K. Xu, Critical pH and exchangeable Al of four acidic soils derived from different parent materials for maize crops, J. Soils Sediments 18 (4) (2018) 1490–1499, https://doi.org/10.1007/s11368-017-1887-x.

[27] G.S. Liu, Soil Physical-Chemical Analysis and Soil Profile Description Methods, Standards Press of China, Beijing, 2000.

[28] W.W. Wenzel, N. Kirchbaumer, T. Prohaska, G. Stingeder, E. Lombi, D.C. Adriano, Arsenic fractionation in soils using an improved sequential extraction procedure, Anal. Chim. Acta 436 (2) (2001) 309–323, https://doi.org/10.1016/S0003-2670(01)00924-2.

[29] C. Ding, Y. Ma, X. Li, T. Zhang, X. Wang, Derivation of soil thresholds for lead applying species sensitivity distribution: a case study for root vegetables, J. Hazard Mater. 303 (2016) 21–27, https://doi.org/10.1016/j.jhazmat.2015.10.027.

[30] G. De'ath, Boosted trees for ecological modeling and prediction, Ecology 88 (1) (2007) 243–251, https://doi.org/10.1890/0012-9658(2007)88[243:btfema]2.0.co;2.

[31] F. Gao, Y. Shen, J.B. Sallach, H. Li, W. Zhang, Y. Li, et al., Predicting crop root concentration factors of organic contaminants with machine learning models, J. Hazard Mater. 424 (2022) 127437, https://doi.org/10.1016/j.jhazmat.2021.127437.

[32] G. Wu, C. Kechavarzi, X. Li, S. Wu, S.J. Pollard, H. Sui, et al., Machine learning models for predicting PAHs bioavailability in compost amended soils, Chem. Eng. J. 223 (2013) 747–754, https://doi.org/10.1016/j.cej.2013.02.122.

[33] T. Wu, C. Liu, P. Cui, H. Zhang, S. Hu, P. Zhang, et al., Kinetics of coupled sorption and abiotic oxidation of antimony (III) in soils, Geoderma 434 (2023) 116486, https://doi.org/10.1016/j.geoderma.2023.116486.

[34] X. Huang, X. Li, L. Zheng, Y. Zhang, L. Sun, Y. Feng, et al., Comprehensive assessment of health and ecological risk of cadmium in agricultural soils across China: a tiered framework, J. Hazard Mater. 465 (2024) 133111, https://doi.org/10.1016/j.jhazmat.2023.133111.

[35] J. Song, F.-J. Zhao, S.P. McGrath, Y.-M. Luo, Influence of soil properties and aging on arsenic phytotoxicity, Environ. Toxicol. Chem. 25 (6) (2006) 1663–1670, https://doi.org/10.1897/05-480r2.1.

[36] Y. Wang, X. Zeng, Y. Lu, L. Bai, S. Su, C. Wu, Dynamic arsenic aging processes and their mechanisms in nine types of Chinese soils, Chemosphere 187 (2017) 404–412, https://doi.org/10.1016/j.chemosphere.2017.08.086.

[37] R.-Q. Huang, S.-F. Gao, W.-L. Wang, S. Staunton, G. Wang, Soil arsenic availability and the transfer of soil arsenic to crops in suburban areas in Fujian Province, southeast China, Sci. Total Environ. 368 (2–3) (2006) 531–541, https://doi.org/10.1016/j.scitotenv.2006.03.013.

[38] C. Ding, T. Zhang, X. Wang, F. Zhou, Y. Yang, G. Huang, Prediction model for cadmium transfer from soil to carrot (Daucus carota L.) and its application to derive soil thresholds for food safety, J. Agric. Food Chem. 61 (43) (2013) 10273–10282, https://doi.org/10.1021/jf4029859.

[39] Y.N. Wan, B. Jiang, D.P. Wei, Y.B. Ma, Ecological criteria for zinc in Chinese soil as affected by soil properties, Ecotoxicol, Environ. Saf. 194 (2020), https://doi.org/10.1016/j.ecoenv.2020.110418.

[40] X. Wang, D. Wei, Y. Ma, M.J. McLaughlin, Derivation of soil ecological criteria for copper in Chinese soils, PLoS One 10 (7) (2015) e0133941, https://doi.org/10.1371/journal.pone.0133941.

[41] M. Kader, D.T. Lamb, M. Megharaj, R. Naidu, Sorption parameters as a predictor of arsenic phytotoxicity in Australian soils, Geoderma 265 (2016) 103–110, https://doi.org/10.1016/j.geoderma.2015.11.019.

[42] A.G. Ilgen, J.N. Kruichak, K. Artyushkova, M.G. Newville, C. Sun, Redox transformations of as and Se at the surfaces of natural and synthetic ferric nontronites: role of structural and adsorbed Fe (II), Environ. Sci. Technol. 51 (19) (2017) 11105–11114, https://doi.org/10.1021/acs.est.7b03058.

[43] Q. Zheng, J. Hou, W. Hartley, L. Ren, M. Wang, S. Tu, et al., As (III) adsorption on Fe-Mn binary oxides: are Fe and Mn oxides synergistic or antagonistic for arsenic removal? Chem. Eng. J. 389 (2020) 124470 https://doi.org/10.1016/j.cej.2020.124470.

[44] K. Amstaetter, T. Borch, P. Larese-Casanova, A. Kappler, Redox transformation of arsenic by Fe (II)-activated goethite (α-FeOOH), Environ. Sci. Technol. 44 (1) (2010) 102–108, https://doi.org/10.1021/es901274s.

[45] C.M. McCann, C.L. Peacock, K.A. Hudson-Edwards, T. Shrimpton, N.D. Gray, K.L. Johnson, In situ arsenic oxidation and sorption by a Fe-Mn binary oxide waste in soil, J. Hazard Mater. 342 (2018) 724–731, https://doi.org/10.1016/j.jhazmat.2018.08.066.

[46] A. Romero-Freire, M. Sierra-Aragon, I. Ortiz-Bernad, F.J. Martin-Peinado, Toxicity of arsenic in relation to soil properties: implications to regulatory purposes, J. Soils Sediments 14 (5) (2014) 968–979, https://doi.org/10.1007/s11368-014-0845-0.

[47] P. Chen, H.-M. Zhang, B.-M. Yao, S.-C. Chen, G.-X. Sun, Y.-G. Zhu, Bioavailable arsenic and amorphous iron oxides provide reliable predictions for arsenic transfer in soil-wheat system, J. Hazard Mater. 383 (2020) 121160, https://doi.org/10.1016/j.jhazmat.2019.121160.

[48] S.C. Maguffin, L. Abu-Ali, R.V. Tappero, J. Pena, J.S. Rohila, A.M. McClung, et al., Influence of manganese abundances on iron and arsenic solubility in rice paddy soils, Geochem. Cosmochim. Acta 276 (2020) 50–69, https://doi.org/10.1016/j.gca.2020.02.012.

[49] J. Dai, C. Chen, A.-X. Gao, Z. Tang, P.M. Kopittke, F.-J. Zhao, et al., Dynamics of dimethylated monothioarsenate (DMMTA) in paddy soils and its accumulation in rice grains, Environ. Sci. Technol. 55 (13) (2021) 8665–8674, https://doi.org/10.1021/acs.est.1c00133.

[50] Y. Hashimoto, Y. Kanke, Redox changes in speciation and solubility of arsenic in paddy soils as affected by sulfur concentrations, Environ. Pollut. 238 (2018) 617–623, https://doi.org/10.1016/j.envpol.2018.03.039.

[51] E. Arco-Lázaro, I. Agudo, R. Clemente, M.P. Bernal, Arsenic (V) adsorption-desorption in agricultural and mine soils: effects of organic matter addition and phosphate competition, Environ. Pollut. 216 (2016) 71–79, https://doi.org/10.1016/j.envpol.2016.05.054.

[52] K. Gupta, A. Srivastava, S. Srivastava, A. Kumar, Phyto-genotoxicity of arsenic contaminated soil from Lakhimpur Kheri, India on Vicia faba L, Chemosphere 241 (2020) 125063, https://doi.org/10.1016/j.chemosphere.2019.125063.

[53] Z. Wu, H. Ren, S.P. McGrath, P. Wu, F.-J. Zhao, Investigating the contribution of the phosphate transport pathway to arsenic accumulation in rice, Plant Physiol. 157 (1) (2011) 498–508, https://doi.org/10.1104/pp.111.178921.

[54] A.M. Mawia, S. Hui, L. Zhou, H. Li, J. Tabassum, C. Lai, et al., Inorganic arsenic toxicity and alleviation strategies in rice, J. Hazard Mater. 408 (2021) 124751, https://doi.org/10.1016/j.jhazmat.2020.124751.

[55] J. Wu, J. Liang, L.O. Björn, J. Li, W. Shu, Y. Wang, Phosphorus-arsenic interaction in the 'soil-plant-microbe' system and its influence on arsenic pollution, Sci. Total Environ. 802 (2022) 149796, https://doi.org/10.1016/j.scitotenv.2021.149796.

[56] M.G. Paoletti, The role of earthworms for assessment of sustainability and as bioindicators, Agric. Ecosyst. Environ. 74 (1–3) (1999) 137–155, https://doi.org/10.1016/S0167-8809(99)00034-1.

[57] H.-T. Wang, D. Zhu, G. Li, F. Zheng, J. Ding, P.J. O'Connor, et al., Effects of arsenic on gut microbiota and its biotransformation genes in earthworm Metaphire sieboldi, Environ. Sci. Technol. 53 (7) (2019) 3841–3849, https://doi.org/10.1021/acs.est.8b06695.

[58] H.-T. Wang, L. Ma, D. Zhu, J. Ding, G. Li, B.-J. Jin, et al., Responses of earthworm Metaphire vulgaris gut microbiota to arsenic and nanoplastics contamination, Sci. Total Environ. 806 (2022) 150279, https://doi.org/10.1016/j.scitotenv.2021.150279.

[59] Z. Wang, Z. Cui, Accumulation, biotransformation, and multi-biomarker responses after exposure to arsenic species in the earthworm Eisenia fetida, Toxicol. Res-UK. 5 (2) (2016) 500–510, https://doi.org/10.1039/c5tx00396b.

[60] Z. Wang, Z. Cui, L. Liu, Q. Ma, X. Xu, Toxicological and biochemical responses of the earthworm Eisenia fetida exposed to contaminated soil: effects of arsenic species, Chemosphere 154 (2016) 161–170, https://doi.org/10.1016/j.chemosphere.2016.03.070.

[61] T. Li, Q. Zhou, The key role of Geobacter in regulating emissions and biogeochemical cycling of soil-derived greenhouse gases, Environ. Pollut. 266 (2020) 115135, https://doi.org/10.1016/j.envpol.2020.115135.

[62] J.-H. Huang, Impact of microorganisms on arsenic biogeochemistry: a review, Water, Air, Soil Pollut 225 (2014) 1–25, https://doi.org/10.1007/s11270-013-1848-y.

[63] S.-L. Tsai, S. Singh, W. Chen, Arsenic metabolism by microbes in nature and the impact on arsenic remediation, Curr. Opin. Biotechnol. 20 (6) (2009) 659–667, https://doi.org/10.1016/j.copbio.2009.09.013.

[64] Z. Wang, H. Tian, X. Tan, F. Wang, H. Jia, M. Megharaj, et al., Long-term as contamination alters soil enzyme functional stability in response to additional heat disturbance, Chemosphere 229 (2019) 471–480, https://doi.org/10.1016/j.chemosphere.2019.05.055.

[65] Z. Wang, H. Tian, M. Lei, M. Megharaj, X. Tan, F. Wang, et al., Soil enzyme kinetics indicate ecotoxicity of long-term arsenic pollution in the soil at field scale, Ecotoxicol. Environ. Saf. 191 (2020) 110215, https://doi.org/10.1016/j.ecoenv.2020.110215.

[66] T. Mehmood, I. Bibi, M. Shahid, N.K. Niazi, B. Murtaza, H. Wang, et al., Effect of compost addition on arsenic uptake, morphological and physiological attributes of maize plants grown in contrasting soils, J. Geochem. Explor. 178 (2017) 83–91, https://doi.org/10.1016/j.gexplo.2017.03.018.

[67] B. Gong, E. He, H. Qiu, C.A. Van Gestel, A. Romero-Freire, L. Zhao, et al., Interactions of arsenic, copper, and zinc in soil-plant system: partition, uptake and phytotoxicity, Sci. Total Environ. 745 (2020) 140926, https://doi.org/10.1016/j.scitotenv.2020.140926.

[68] S. Zhao, L. Qin, L. Wang, X. Sun, L. Yu, M. Wang, et al., Ecological risk thresholds for Zn in Chinese soils, Sci. Total Environ. 833 (2022) 155182, https://doi.org/10.1016/j.scitotenv.2022.155182.

[69] Y. Liu, J. Yu, H. Sun, T. Li, X. He, Z. Lin, Screening and prioritizing substances in groundwater in the Beijing–Tianjin–Hebei region of the North China Plain based on exposure and hazard assessments, J. Hazard Mater. 423 (2022) 127142, https://doi.org/10.1016/j.jhazmat.2021.127142.

[70] A. Baker, P.L. Walker, Physiological responses of plants to heavy metals and the quantification of tolerance and toxicity, Chem. Speciat. Bioavailab. 1 (1) (1989) 7–17, https://doi.org/10.1080/09542299.1989.11083102.

[71] A. Del Signore, A.J. Hendriks, H.R. Lenders, R.S. Leuven, A. Breure, Development and application of the SSD approach in scientific case studies for ecological risk assessment, Environ. Toxicol. Chem. 35 (9) (2016) 2149–2161, https://doi.org/10.1002/etc.3474.

[72] L. Qin, X. Sun, L. Yu, J. Wang, S. Modabberi, M. Wang, et al., Ecological risk threshold for Pb in Chinese soils, J. Hazard Mater. 444 (2023) 130418, https://doi.org/10.1016/j.jhazmat.2022.130418.